

Establishment of BCWM.1 cell line for Waldenström's macroglobulinemia with productive *in vivo* engraftment in SCID-hu mice

Daniel Ditzel Santos^{a,b}, Allen W. Ho^{a,c}, Olivier Tournilhac^{a,b},
Evdoxia Hatjiharissi^{a,b}, Xavier Leleu^{a,b}, Lian Xu^a, Pierfrancesco Tassone^{a,c,d},
Paola Neri^{a,c,d}, Zachary R. Hunter^a, Mariana A.Z. Chemaly^a, Andrew R. Branagan^a,
Robert J. Manning^a, Christopher J. Patterson^a, Anne Sophie Moreau^{a,b}, Bryan Ciccarelli^a,
Sophia Adamia^{a,e}, Jitra Kriangkum^e, Jeffery L. Kutok^b, Yu-Tzu Tai^{a,b}, Jiangwen Zhang^f,
Linda M. Pilarski^e, Kenneth C. Anderson^b, Nikhil Munshi^{b,c}, and Steven P. Treon^{a,b}

^aBing Center for Waldenström's Macroglobulinemia, Dana-Farber
Cancer Institute, Boston, Mass., USA; ^bDepartment of Medicine, Harvard Medical
School, Boston, Mass., USA; ^cVA Boston Healthcare System, Boston, Mass., USA; ^dUniversity
of "Magna Græcia" and Cancer Center, Catanzaro, Italy; ^eDepartment of Oncology, University of Alberta,
Cross Cancer Institute, Edmonton, Alberta, Canada; ^fFAS Center for Systems Biology, Harvard University, Cambridge Mass., USA

(Received 31 March 2007; revised 23 May 2007; accepted 31 May 2007)

A significant impairment in understanding the biology and advancing therapeutics for Waldenström's macroglobulinemia (WM) has been the lack of a representative cell line and animal model. We, therefore, report on the establishment of the BCWM.1 cell line, which was derived from the long-term culture of CD19⁺ selected bone marrow lymphoplasmacytic cells isolated from an untreated patient with WM. BCWM.1 cells morphologically resemble lymphoplasmacytic cells (LPC) and propagate in RPMI-1640 medium supplemented with 10% fetal bovine serum. Phenotypic characterization by flow cytometric analysis demonstrated typical WM LPC characteristics: CD5⁻, CD10⁻, CD19⁺, CD20⁺, CD23⁺, CD27⁻, CD38⁺, CD138⁺, CD40⁺, CD52⁺, CD70⁺, CD117⁺, cIgM⁺, cIgG⁻, cIgA⁻, cκ⁻, cλ⁺, as well as the survival proteins APRIL and BLYS, and their receptors TACI, BCMA and BAFF-R. Enzyme-linked immunosorbent assay studies demonstrated secretion of IgMλ and soluble CD27. Karyotypic and multicolor fluorescence *in situ* hybridization studies did not demonstrate cytogenetic abnormalities. Molecular analysis of BCWM.1 cells confirmed clonality by determination of IgH rearrangements. Inoculation of BCWM.1 cells in human bone marrow chips implanted in severe combined immunodeficient-hu mice led to rapid engraftment of tumor cells and serum detection of human IgM, λ, and soluble CD27. These studies support the use of BCWM.1 cells as an appropriate model for the study of WM, which in conjunction with the severe combined immunodeficient-hu mouse model may be used as a convenient model for studies focused on both WM pathogenesis and development of targeted therapies for WM. © 2007 ISEH - Society for Hematology and Stem Cells. Published by Elsevier Inc.

Waldenström's macroglobulinemia (WM) is an incurable B-cell malignancy primarily characterized by bone marrow infiltration with lymphoplasmacytic cells (LPC), along with demonstration of an IgM monoclonal gammopathy [1].

Offprint requests to: Steven P. Treon, M.D., M.A., Ph.D., Bing Center for Waldenström's Macroglobulinemia, Dana Farber Cancer Institute, M547/8, 44 Binney Street, Boston, MA 02115 USA; E-mail: steven_treon@dfci.harvard.edu

The underlying pathological disorder for WM is considered to be lymphoplasmacytic lymphoma as defined by the Revised European-American Lymphoma and World Health Organization classification systems [2,3]. A strong familial predisposition has been reported in WM, with up to 20% of patients demonstrating a first-degree relative with WM or a closely related B-cell malignancy [4].

Several studies have been published on cytogenetic findings in WM, with deletions of chromosome 6q21-22

constituting the most widely reported cytogenetic abnormality. Deletions in 6q21-22 have been observed in half of WM patients, irrespective of familial history, and may help discriminate WM from IgM monoclonal gammopathy of undetermined significance [4–6]. Several candidate tumor suppressor genes in this region are under study, including BLIMP-1, a master regulatory gene implicated in lymphoplasmacytic differentiation and genes downstream of BLIMP-1, including PAX-5, XBP-1, and the XBP-1 splicing protein IRE-1 [7,8]. A consistent finding in the genetic studies of WM has been the absence of IgH region switch rearrangements, a finding that may be used to discern cases of IgM myeloma where IgH region switch rearrangements are a predominant feature [9]. A strong preferential usage of VH3/JH4 gene families, without intraclonal variation and isotype-switched transcripts has also been reported in WM [10,11], suggesting that WM may have originated from a IgM⁺ and/or IgM⁺ IgD⁺ memory B cell.

The phenotype of LPC in WM cell further suggests that the malignant clone is likely to represent a postgerminal center B cell. LPC in WM express cell surface CD19, CD20, CD22, CD52, IgM, IgD, as well as the activation markers CD25, CD38, CD40, and CD70 [12–15]. Variably, WM LPC may also express CD5, CD10, CD23 [16]. Normally CD27 is expressed on the cell surface of memory B cells from which the WM clone is thought to derive. However, in WM, CD27 is heterogeneously expressed, and more often is absent on the cell surface of WM LPC [11,12,14]. In addition, WM LPC widely express the tumor necrosis factor family members B-lymphocyte stimulator protein and a proliferation-inducing ligand (APRIL) as well as their receptors, which may provide growth and survival signals [17–20]. Lastly, WM cells secrete both IgM and soluble CD27 (sCD27), both of which serve as markers of disease burden in WM [19,20]. Importantly, sCD27 may also have an important biological role in WM pathogenesis by inducing the growth and survival factors APRIL and CD40L on mast cells, which are found in increased number in the bone marrow (BM) of patients and support the expansion of WM cells [19–24].

A significant impairment in understanding the biology and advancing therapeutics for WM has been the lack of representative cell lines and an animal model. In this study, we report on the establishment of a cell line that demonstrates typical cytogenetic, morphological, and phenotypic features of WM, and that readily engrafts and provides a representative model of WM disease in severe combined immunodeficient (SCID)-hu mice.

Materials and methods

Case description

In April 2004, a previously untreated female patient presented with complaints of headaches, blurry vision, lethargy, persistent

sweating, bilateral hand tingling, nose bleeds, easy bruising, leg cramps, diffuse joint pain, and frequent sinus infections with no concomitant loss of weight. Her social history was unremarkable for cigarette smoking, alcohol use, or occupational exposures. Likewise, her family history was unremarkable for any malignancy or other B-cell disorder. On physical examination, she demonstrated no adenopathy or hepatosplenomegaly. Laboratory tests demonstrated normocytic anemia, along with a normal white blood and platelet count. Electrolytes and liver function tests were within normal limits. Serum IgM level at time of evaluation was 4430 (normal range, 40–230 mg/dL), and serum viscosity was 2.5 (normal range, 1.4–1.8 CP). Moreover, as is typical of WM, IgG and IgA levels were subnormal at 676 (range, 700–1600 mg/dL) and 26 (range, 70–400 mg/dL), respectively [25]. β 2-microglobulin, a prognostic factor in WM, was normal at 1.8 mg/dL [15]. Both antimyelin-associated glycoprotein and ganglioside M1 antibodies obtained as part of a workup for an IgM-related neuropathy were not present. A bone marrow biopsy demonstrated 5% intertrabecular space involvement with lymphoplasmacytic cells consistent with the Revised European-American Lymphoma/World Health Organization pathological diagnosis of lymphoplasmacytic lymphoma [2,3]. By flow cytometric analysis, LPC coexpressed CD19, CD20, and CD52, and were negative for CD5, CD10, and CD11c. Serological studies were unremarkable for hepatitis B, C, and HIV, but demonstrated remote infection with Epstein-Barr virus.

Isolation of BCWM.1 WM cells

A BM aspirate was obtained for these studies following informed consent, and with the approval of our Institutional Review Board. The patient was newly diagnosed and untreated at time the BM aspirate was obtained. Mononuclear cells from the BM aspirate were isolated by density-gradient centrifugation using Ficoll-Paque Plus-1070 (Pharmacia Biotech, Piscataway, NJ, USA). LPC immunoselection was performed using a CD19⁺ cell isolation kit (Miltenyi Biotec, Auburn, CA, USA) according to the manufacturer's instructions. Following CD19⁺ isolation, >90% of cells coexpressed CD20. LPCs were then cultured in Stem Pro 34 serum-free media (Life Technologies, Grand Island, NY, USA), supplemented with 2 mM L-glutamine (Mediatech, Cellgro, AK, USA), 100 U/mL penicillin, 10 μ g streptomycin (Mediatech), and stem cell factor at 100 ng/mL (Amgen, Thousand Oaks, CA, USA), given that 96% of cells expressed CD117. Expanded cells were doubled every 3 days for the first 4 months of culture. At 4 months, cells were subcultured in RPMI-1640 plus 10% heat-inactivated fetal bovine serum, with 2 mM L-glutamine (Mediatech), 100 U/mL penicillin and 10 μ g streptomycin (Mediatech). In this new culture environment, the cell line maintained the same proliferation rate as well as morphological characteristics. A subculture was then established from a single cell clone isolated from cell sorting with a FC500 Analyzer (Beckman Coulter, Miami, FL, USA).

Morphological characterization of BCWM.1 cells

Morphological assessment was performed by a cytopathologist following Giemsa staining of cytopins. For electron microscopic analysis, cells were fixed in 2% paraformaldehyde/2.5% glutaraldehyde in 0.1 M sodium cacodylate buffer, at a pH of 7.4 for 1 hour at room temperature; postfixed in 1% osmium tetroxide/1.5% potassium ferrocyanide in water for 30 minutes; and then

stained in 1% uranyl acetate in maleate buffer pH 5.2 for 30 minutes at room temperature. After dehydration in graduated ethanols (70%, 95%, and 2 × 100%), cells were removed from the dish, placed in propylene oxide, and centrifuged at 3000 rpm for 3 minutes. Pellets were suspended in a 1:1 mixture of propylene oxide and Epon (TAAB Epon, Marivac Ltd, Nova Scotia, Canada) for 2 hours at room temperature, transferred to embedding molds filled with pure TAAB Epon, and polymerized for 48 hours at 60°C. Ultrathin sections (80–90 nm) were mounted on copper grids, stained with 2% uranyl acetate in acetone followed by 0.2% lead citrate, and then examined in a JEOL 1200EX transmission electron microscope, as described previously [12].

Phenotypic characterization of BCWM.1 cells

Multicolor flow cytometric analysis was performed using FC500 Analyzer. Staining patterns for all antibodies used were compared to their respective isotype control. The following antibodies were used: CD5, CD9, CD10, CD11a, CD11c, CD19, CD20, CD22, CD25, CD23, CD30, CD34, CD38, CD66b, CD80, IgM, IgG, IgD, CD138, FMC7, and CD40, all conjugated to PC5 (BD Biosciences, San Jose, CA, USA); CD4, CD8, CD14, CD16, CD27, CD56 (Beckman Coulter, Miami, FL, USA), CD70 (RDI, Flanders, NJ, USA); CD52 (Serotec Inc., Raleigh, NC, USA), anti-FcεRIα (Upstate, Lake Placid, NY, USA), all conjugated to fluorescein isothiocyanate (Pharmacia); BlyS (eBioscience, San Diego, CA, USA); TACI (R & D Systems, Minneapolis, MN, USA), BCMA (Axxora, San Diego, CA, USA), and BR3 (Genentech BioOncology, Inc., San Francisco, CA, USA), all conjugated to phycoerythrin (Pharmacia); and CD117, conjugated to PerCP-Cy5.5. Antigen expression was deemed positive if ≥20% of cells demonstrated specific binding. Intracellular staining was also analyzed for immunoglobulins and light chain presence following membrane permeabilization.

Reverse transcriptase polymerase chain reaction analysis for APRIL, BLYS, and their receptors

Total RNA was extracted from 1–5 × 10⁶ LPCs and 0.2–1 × 10⁶ MCs using RNeasy Mini Kit (Qiagen, Valencia, CA, USA). The 0.3 μg RNA was reverse transcribed in a 20 μL reaction by oligo-p-(dT)₁₅ priming using Superscript III reverse transcriptase according to the protocol provided by Invitrogen. First-strand cDNA was synthesized using Superscript III reverse transcriptase according to the protocol also provided by Invitrogen. Two microliters first-strand cDNA was used as template for PCR amplification. PCR was performed using the PTC-200 DNA Engine Thermal Cycler (MJ Research Inc., Waltham, MA, USA). The pool of primers used in these experiments was as follows: BCMA (sense): 5'-TAA CTT GTC CTT CCA GGC TGT TCT-3'; BCMA (antisense): 5'-CAT AGA AAC CAA GGA AGT TTC TAC C-3'; TACI (sense): 5' CAC CCT AAG CAA TGT GC-3'; TACI (antisense): 5'- TGG GAC TCA GAG TGC C -3'; BAFF_R (sense): 5'- AAT CTC TGA TGC CAC AGC TCC TGC -3'; BAFF_R (antisense): 5'- TCA AAG ATG GTG AGG TCT GAA GCC -3'; BlyS (sense): 5' TCA GGG TCC AGA AGA AAC AGT C 3'; BlyS (antisense): 5' GCT ACA GAC ATG GTG TAA GTA GG 3'; APRIL (sense): 5'-CCT TGC TAC CCC ACT CTT G-3'; APRIL (antisense): 5'-ACA CTC AGA ATA TCC CCT TGG-3'. After an initial denaturation, glyceraldehyde phosphate dehydrogenase amplification was performed. The amplified fragments were stained with 0.3 mg/mL ethidium bromide (Sigma, St Louis, MO, USA) and detected by electrophoresis in 2% (w/v) agarose gel.

Cytogenetic analysis of BCWM.1 cells

Cytogenetic studies of BCWM.1 cells were performed using conventional GTG and both metaphase and interphase fluorescence in situ hybridization (FISH). FISH analyses were performed using the bacterial artificial chromosome probes RP11-79L7, RP11-91C23, RP11-171J20, which hybridize to 6q21, 6q21-22, and

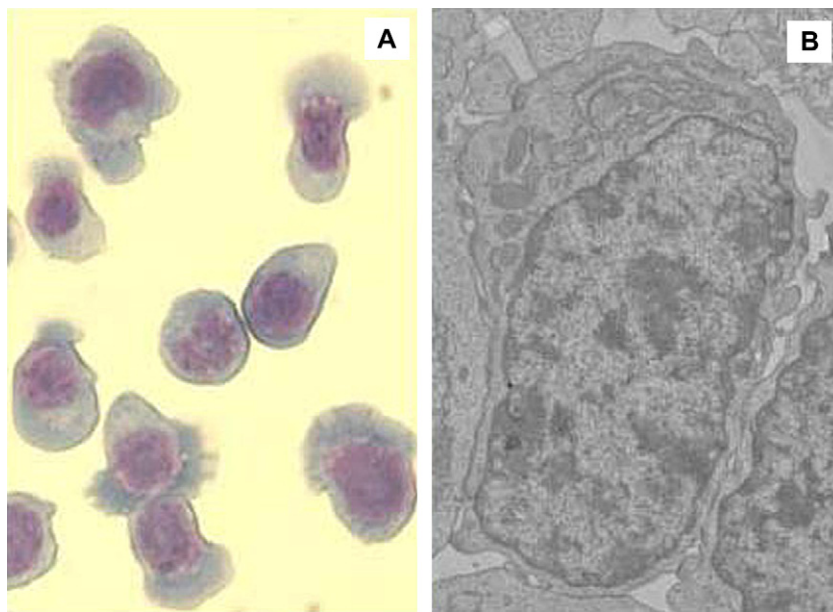


Figure 1. Morphology of BCWM.1 cells discerned at 400× magnification following Giemsa staining under light microscopy (A) and under electron microscopy at 5000× (B) demonstrating typical features of lymphoplasmacytic cells.

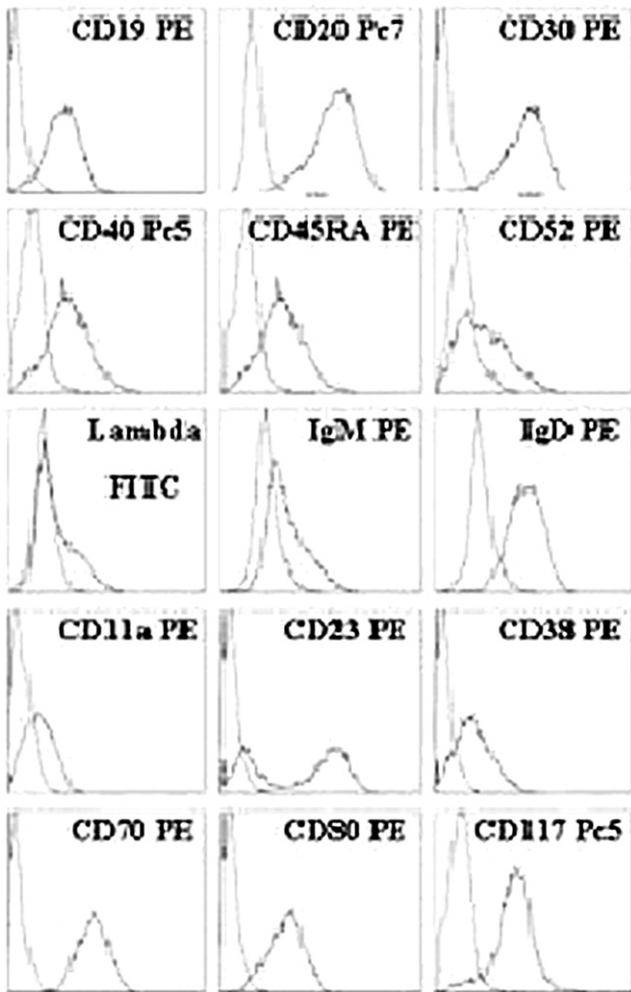


Figure 2. Immunophenotypic characterization of BCWM.1 cells by flow cytometric analysis. First peak represents isotype staining, whereas second peak demonstrates antigen-specific staining for select B-cell surface differentiation and activation antigens.

6q22.1, respectively, and CEP6, which hybridizes to the centromere of chromosome 6 (Children's Hospital Oakland Research Institute) as before [4]. One-hundred cells were counted, and detection of the 6q21-22 deletion was deemed to be positive when $\geq 5\%$ and $\geq 6\%$ of the cells showed loss of hybridization to RP11-91C23 and RP11171J20, and RP11-79L7, respectively [4].

Assessment of clonality by DNA

fragment analysis of IgH V/D/J rearrangements

Genomic DNA from BCWM.1 cells was prepared by the Trizol method (Invitrogen) according to manufacturer's instructions. Rearranged IgH V/D/J segments were amplified from 20 to 80 μg genomic DNA template using 5'hexachloro-fluorescein phosphoramidite labeled FR1c (5'GGTGCAGCTG(G/C)(A/T)G(G/C)AGTC(G/A/T)GG3') and JHc (5'ACCTGAGGAGACGGTGACC(A/G)(G/T)(G/T)GT3') primers as before [11]. The PCR product was mixed with formamide and size standard (GeneScan-500, Applied Biosystems, Foster City, CA, USA), and then analyzed on an ABI

Prism 3100 Genetic Analyzer (Applied Biosystems) according to manufacturer's instructions. Data analysis was performed using GeneMapper software version 3.5.

Gene array analysis of BCWM.1 cells

Total RNA was extracted from BCWM.1 cells and CD19⁺ selected mononuclear cells obtained from healthy donors using the RNeasy Mini Kit (Qiagen). Two to five micrograms extracted RNA were used to generate a cRNA probe by T7 transcription. Fragmented cRNA was then hybridized on human HG-U133 Plus 2 oligonucleotide probe arrays (Affymetrix, Santa Clara, CA, USA) for analysis of mRNA expression levels corresponding to 22,284 transcripts. Arrays were prepared and processed according to manufacturer's directions. The arrays were scanned using the Gene Array scanner (Affymetrix), and the raw intensity. CEL files were normalized with R/Bioconductor software affy package. Bioconductor limma package was used to identify differentially expressed genes. Genes with fold change above 1.5 and *p* value (multitest adjusted) $< 5\%$ were chosen for further analysis, such as pathway enrichment and Gene Ontology classification analysis. All arrays were performed twice in independent experiments.

SNP array analysis

The extraction of genomic DNA from the founding patient's sorted primary lymphoplasmacytic cells and BCWM.1 cells was performed using QIAamp DNA Extraction Kit (Qiagen) according to manufacturer's instructions. The Affymetrix gene chip mapping 500K array (Sty I and Nsp I arrays) was used according to manufacturer's instructions at the Microarray Core Facility, Dana-Farber Cancer Institute, Harvard Medical School (Boston, MA, USA). SNP expression was analyzed with dChipSNP Software. Inferred chromosome copy number changed to 3 or 1 was considered a significant amplification or deletion.

In vivo engraftment of BCWM.1 cells in SCID-hu mice

Six- to eight-week-old male CB-17 SCID mice (Taconic, NY, USA) were housed and monitored in our Animal Research Facility. All experimental procedures and protocols were approved by the Institutional Animal Care and Use Committee (VA Boston Healthcare System). Human fetal long bone grafts (SCID-hu) were implanted into SCID mouse as described previously [26]. Briefly, SCID mice were surgically implanted with human bone chips from fetal femurs or tibia obtained at 19 to 23 weeks gestation. Approximately 4 weeks after implantation, 2.75×10^6 BCWM.1 cells suspended in 50 μL phosphate-buffered saline were injected directly into human fetal bone implants within SCID-hu mice. Increasing levels of circulating human paraprotein in mice sera were used to monitor tumor engraftment and growth of BCWM.1 cells in SCID-hu mice. Peripheral blood from mice was serially collected from tail veins and serum tested for circulating human IgM, IgG, κ and λ light chain by enzyme-linked immunosorbent assay (ELISA; Bethyl Inc., Montgomery, TX, USA), as described previously [26]. ELISA kits used reacted specifically with human immunoglobulins, and did not cross-react with murine immunoglobulins. In some experiments, soluble CD27 was also assessed by ELISA (Bender Medsystems, Burlingame, CA, USA). Fetal bone chips and murine femurs were assessed for BCWM.1 engraftment by histological examination, and assessment by

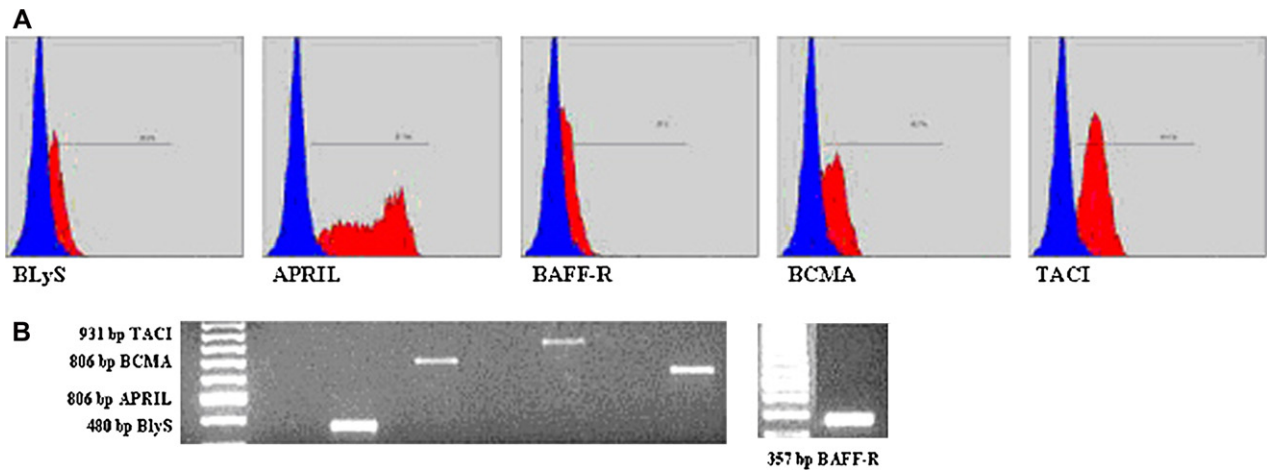


Figure 3. Expression of BLYS, APRIL, and their receptors (BCMA, TACI, BAFF-R) by flow cytometric (A) and reverse transcriptase polymerase chain reaction analysis (B) in BCWM.1 cells.

immunohistochemistry by staining with antibodies for human CD20, IgM, IgG, IgA, κ and λ .

Assays for detection of human immunoglobulin and soluble CD27 secretion

In vitro supernatants from cultures of BCWM.1 cells and murine sera obtained from BCWM.1 engrafted SCIF-hu mice were evaluated by ELISA kits for detection of human IgM (Zeptometrix, Buffalo, NY, USA), human κ and λ light chains (Bethyl Inc., Montgomery, TX, USA), and soluble CD27 (Bender Medsystems).

Assessment for mycoplasma and Epstein Barr virus infection

BCWM.1 cells were evaluated for mycoplasma infection using a mycoplasma detection kit (Roche Diagnostics Corporation, IN, USA). BCWM.1 cells were also evaluated for Epstein-Barr virus

infection by immunohistochemical staining (R&D Systems) and RT-PCR analysis for latent membrane protein 1.

Results

Growth and morphological characteristics of BCWM.1 cells

At an optimum concentration of $0.5\text{--}1.0 \times 10^6$ cells/mL, BCWM.1 cells demonstrated a doubling time of 3 days in RPMI medium supplemented with 10% fetal bovine serum, antibiotics and L-glutamine. BCWM.1 was morphologically characterized as a lymphoplasmacyte displaying prominent nucleoli and ample cytoplasm by Giemsa staining under $400\times$ magnification by light microscopy (Fig. 1). By

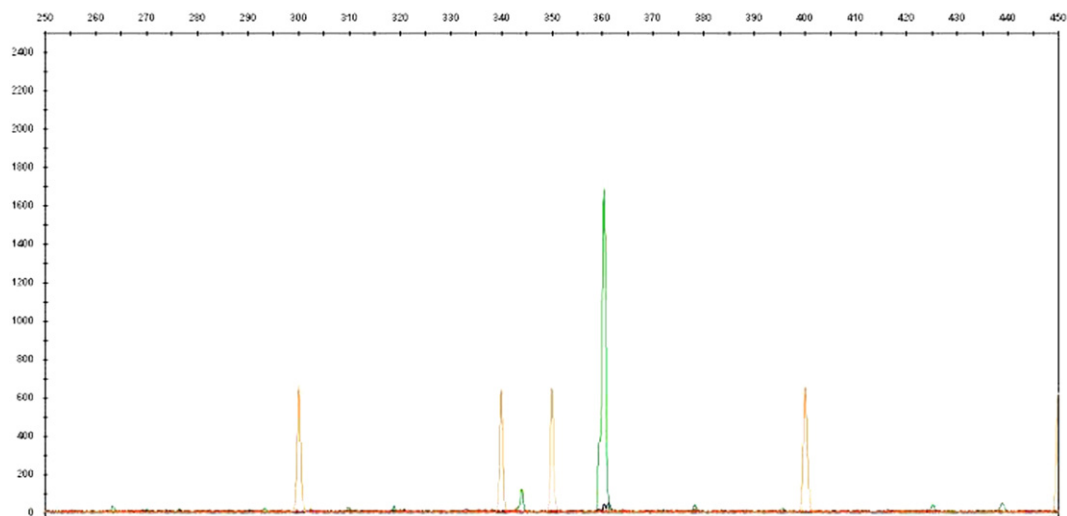


Figure 4. Molecular analysis demonstrating clonality of BCWM.1 cells. Graph shows FR1c/JHc amplification of BCWM.1 genomic DNA analysis. The X-axis represents length of DNA fragment. The green bar is the amplified product demonstrating clonality using FR1c/JHc primers. Orange peaks represent DNA markers.

electron microscopy, the nucleus of BCWM.1 cells showed evenly dispersed chromatin with prominent nucleoli, abundant cytoplasm, organelles, and mitochondria and displayed both short and long profiles of rough endoplasmic reticulum at 5000 \times magnification (Fig. 1). BCWM.1 cells were positive for Epstein-Barr virus latent membrane protein 1 expression by immunohistochemistry and RT-PCR analysis, and negative for mycoplasma infection.

Immunophenotypic characterization of BCWM.1 cells

By flow cytometric analysis, BCWM.1 cells demonstrated the following immunophenotypic characteristics: CD3⁻, CD4⁻, CD5⁻, CD8⁻, CD9⁻, CD10⁻, CD11a⁺, CD11c⁻, CD14⁻, CD16⁻, CD19⁺, CD20⁺, CD22⁻, CD23⁺, CD25⁻, CD27⁻, CD30⁺, CD30L⁻, CD34⁻, CD38⁺, CD40⁺, CD154 (CD40L)⁻, CD45RA⁺, CD45RO⁻, CD52⁺, CD56⁻, CD66b⁻, CD70⁺, CD80⁺, CD103⁻, CD117⁺, CD138⁻, FMC7⁻; positive intracellular staining for cIgM⁺, cIgG⁻, cIgA⁻, c κ ⁻, c λ ⁺ (Fig. 2). BCWM.1 cells also expressed APRIL and B-Lymphocyte Stimulator, as well as the APRIL and BLYS receptors TACI, BCMA, and BAFF-R by flow cytometric and RT-PCR analysis (Fig. 3).

Cytogenetic analysis

Karyotype analysis demonstrated 46 chromosomes, XX, in BCWM.1 cells without cytogenetic anomalies (data not shown). By FISH analysis for the 6q21 deletion, 94 of 100 cells (94%) showed a hybridization pattern consistent with the presence of two copies of this chromosomal locus (data not shown). Greater than 10% of cells with the deletion is considered positive, as previously reported [4].

Molecular analysis for

FR1c/JHc amplification of genomic DNA

Molecular analysis by FR1c/JHc amplification of genomic DNA using single-cell sorting demonstrated a consistent monoclonal peak, thereby establishing clonality for BCWM.1 cells (Fig. 4).

Gene and SNP array analysis

To understand the tumorigenesis mechanism of BCWM.1 cell line, Affymetrix GeneChip Hgu133Plus2 was employed to compare the gene expression profile between BCWM.1 cells (performed in independent duplicate experiments), the founding primary lymphoplasmacytic cells and B cells isolated from the bone marrow of four healthy donors. Genes with fold change > 1.5 and *p* value (multitest adjusted) ≤ 0.05 were considered significant and chosen for further analysis. As shown in Figure 5, gene expression profiling demonstrated considerable overlap between BCWM.1 and the founding patient's primary lymphoplasmacytic cells. However, when BCWM.1 cells were compared by gene expression profiling to normal donor BM B cells for genes relevant in B-cell growth and signaling, 17 genes were significantly up- or downregulated as shown

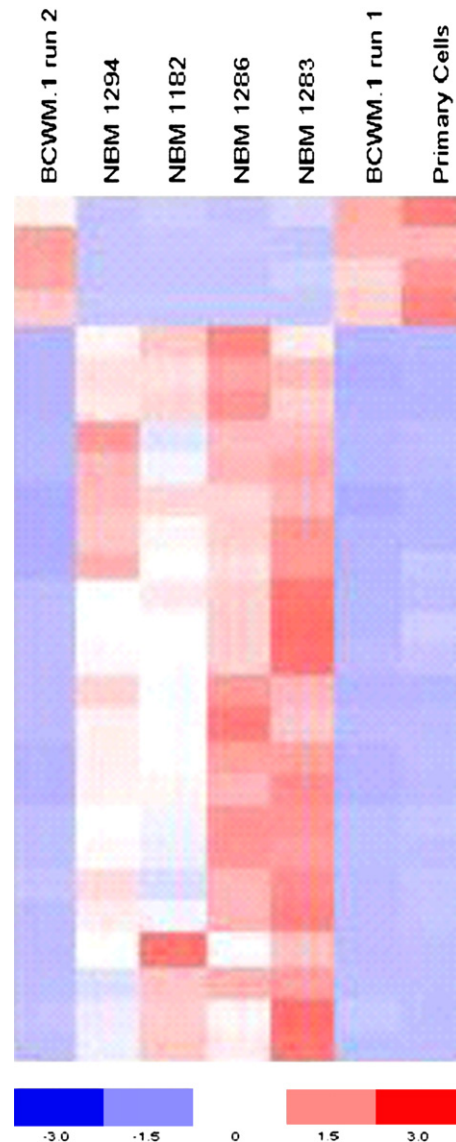


Figure 5. Gene array expression profile for BCWM.1 cells (run in two independent experiments), sorted lymphoplasmacytic cells (CD19⁺) from founder patient and bone marrow B cells (CD19⁺) from four healthy donors.

in Table 1. To detect any potential chromosome changes between BCWM.1 cell line and the founding primary lymphoplasmacytic cells, we also performed 500K SNP array hybridization and analysis. Inferred chromosome copy number change from dChipSNP software revealed a decrease in copy number (to 1) at chromosome 3p14.2 (chr3:60,097,950-60,762,791) when BCWM.1 cells were compared against the founder patient's primary lymphoplasmacytic cells.

In vivo engraftment in SCID-hu mice

We next evaluated the engraftment ability of BCWM.1 cells in five SCID-hu mice by direct subcutaneous injection at 2.75×10^6 cells/mouse. After 30 weeks of observation,

Table 1. Dysregulated genes involved in B-cell homeostasis by comparative gene expression profiling of BCWM.1 vs normal donor bone marrow B cells

Gene	Chromosomal locus	Function	p Value
Downregulated			
Interleukin-6	7p21	B-cell differentiation	0.0003
syk	9q22	B-cell receptor-independent calcium-induced apoptosis	0.0018
Burkitt lymphoma receptor 1, GTP binding protein	11q23	B-cell migration	0.0054
fyn	6q21	Src family tyrosine kinase	0.0124
ζ-chain (TCR) associated protein kinase	2q12	IgM signaling	0.0134
Phospholipase C, β2	15q15	PKC-catalyzed phosphorylation	0.0162
Rho guanine nucleoside exchange factor (GEF) 1	19q13	Erk and PI-3 kinase pathway	0.0267
lef-1	4q23	Wnt signaling, B-cell development	0.0361
Upregulated			
fas (CD95)	10q24	Programmed cell death	0.0018
CASP8 and FADD-like apoptosis regulator	2q33	Programmed cell death	0.0018
Calnexin	5q35	Protein folding and assembly	0.0134
Mitogen-activated protein kinase 7	17p11	TNFR1 signaling pathway	0.0188
p21 (CDKN1A)- activated kinase 2	3q29	Regulation of B-cell proliferation	0.0188
Eukaryotic translation initiation factor 2, subunit 1 α	14q23	Protein synthesis initiation	0.0205
Caspase-1, apoptosis-related cysteine protease	11q23	Programmed cell death	0.0258

no tumor growth occurred, and no human paraprotein was detectable in serum. We subsequently inoculated BCWM.1 at the same concentration in a fetal bone chip, which was implanted in five other SCID-hu mice. Human paraproteins were undetectable at baseline, but were readily detectable in four mice at 2 weeks, and in one mouse at 4 weeks. Importantly, follow-up evaluation at 4 weeks showed both increasing serum IgM and λ-light chain levels in all five mice (Table 2). In a separate pilot study, and under the same conditions, we implanted BCWM.1 inoculated fetal bone chips into five other SCID-hu mice in which both serum IgM and sCD27 levels were followed. Both serum IgM and sCD27 levels were undetectable at baseline, but became readily detectable at 2 weeks and continued to rise to 12 weeks (data not shown).

To ascertain the distribution of engraftment of BCWM.1 cells, as well as the necessity for a human bone marrow environment to support BCWM.1 engraftment, we performed a detailed histological examination of the human and mouse bone marrows by examining decalcified sections of the human fetal bone implanted bone chips and mouse femurs, as well as murine spleens, liver, lung, kidney, and lymph nodes from four SCID-hu mice following 4 weeks of BCWM.1 engraftment. Histological and immunohistochemical evaluation demonstrated the presence of diffuse

lymphoplasmacytic cells in the human bone marrow (Fig. 6), but not murine bone marrow, spleen, liver, lung, or kidney (data not shown) which stained for human CD20, IgM, and λ-light chains but not human IgA, IgG, or κ light chains (Fig. 7).

Discussion

A significant impairment in understanding the biology and advancing novel therapeutics for WM has been the lack of a representative cell line and animal model. We, therefore, report on work accomplished in our laboratories in establishing the BCWM.1 cell line and a SCID-hu mouse model utilizing BCWM.1 cells to recapitulate the biology of WM.

As demonstrated in these studies, BCWM.1 bore the morphological, phenotypic, and genotypic properties of LPC typically found in WM, as well as important biological features, such as the secretion of IgM and sCD27 that serve as surrogate markers of disease in WM [20]. The production of sCD27 may particularly be significant for the pathogenesis of WM, since this ligand induces the growth and survival factors APRIL and CD40L on mast cells, which express the receptor for CD27 (CD70); are increased in number in the BM of patients with WM; and are usually found in close association with LPC [24]. Soluble CD27

Table 2. Serial paraprotein measurements in SCID-hu mice engrafted with BCWM.1 WM cells

Mouse Code	Isotype	Cells ($\times 10^6$) Inoculated	Weeks to IgM detection	Level of IgM ($\mu\text{g/mL}$)		Level of λ- light chain ($\mu\text{g/mL}$)	Level of λ-light chain ($\mu\text{g/mL}$)
				Week 2	Week 4	Week 2	Week 4
680D	IgM λ	2.75	2	9.1	20.1	9.4	23.6
323B	IgM λ	2.75	4	0	12.4	4.6	10.3
NA	IgM λ	2.75	2	54.4	152.6	57.5	114.2
072D	IgM λ	2.75	2	153.7	381.3	115.4	227.2
2D36	IgM λ	2.75	2	20.16	50.4	16.8	35.2

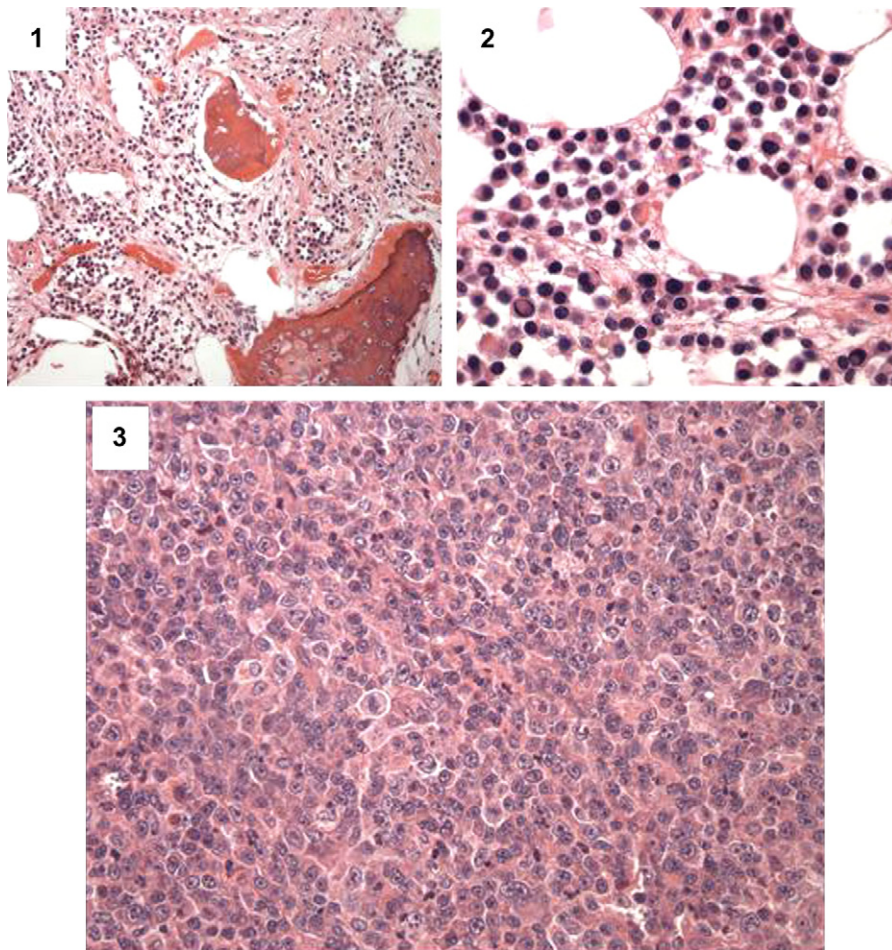


Figure 6. Histological analysis for human bone marrow engraftment in severe combined immunodeficient (SCID)-hu mice with BCWM.1 lymphoplasmacytic cells. Histological analysis was performed on decalcified fetal bone chips implanted in SCID-hu mice following engraftment with BCWM.1 lymphoplasmacytic cells. Bone chips were retrieved from SCID-hu mice at 12 weeks following serial detection of rising human paraproteins in murine serum. Fetal bone chips were then stained with hematoxylin and eosin, and viewed under light microscopy at 100 \times (1), 400 \times (2), and 200 \times (3).

may also have other important roles in WM pathogenesis, including immune suppression [27].

BCWM.1 cells also expressed APRIL and BLYS, as well as their receptors TACI and BCMA (for both APRIL and BLYS) and BAFF-R (for BLYS). Similar findings have been reported by us and others in primary WM LPC [17,18], as well as on malignant cells in other B-cell disorders [28,29]. The expression of both APRIL and BLYS as well as their receptors on WM cells may have important roles in WM pathogenesis, particularly because these ligand-receptor pathways have well-defined roles in LPC differentiation and IgH class switching. The BCWM.1 cell line may therefore provide a convenient model for the regulatory study of APRIL and BLYS in WM.

As part of these studies, we also performed extensive cytogenetic, molecular, and gene expression studies on BCWM.1 cells. These studies confirmed the clonality of BCWM.1 cells by determination of IgH rearrangements through FR1c/JHc amplification of genomic DNA, while SNP-1 analysis demonstrated close propinquity of

BCWM.1 cells to the founder patient's primary LPC, with the sole change being an decrease (to one) in copy number at 3p14.2. Two potential genes of interest at 3p14.2 are the fragile histidine triad gene (FHIT) and the protein tyrosine phosphatase receptor type G gene, both of which are candidate tumor suppressor genes [30]. Aberrant expression of FHIT has been reported in several B-cell malignancies [31,32], and further investigation of both the FHIT and phosphatase receptor type G genes in the pathogenesis and progression of WM would appear warranted. Interestingly, gene expression profiling revealed significant differences in 17 genes with a role in B-cell homeostasis that are worthy of further study in WM, including *fyn*, which is located at 6q21, a site shown by us and others to be frequently deleted in patients with WM, and which may have a role in the progression of IgM MGUS to WM [4–6].

As is typical of primary LPC from most WM patients, no gross structural abnormalities were found in BCWM.1 cells by karyotype and multicolor fluorescence in situ

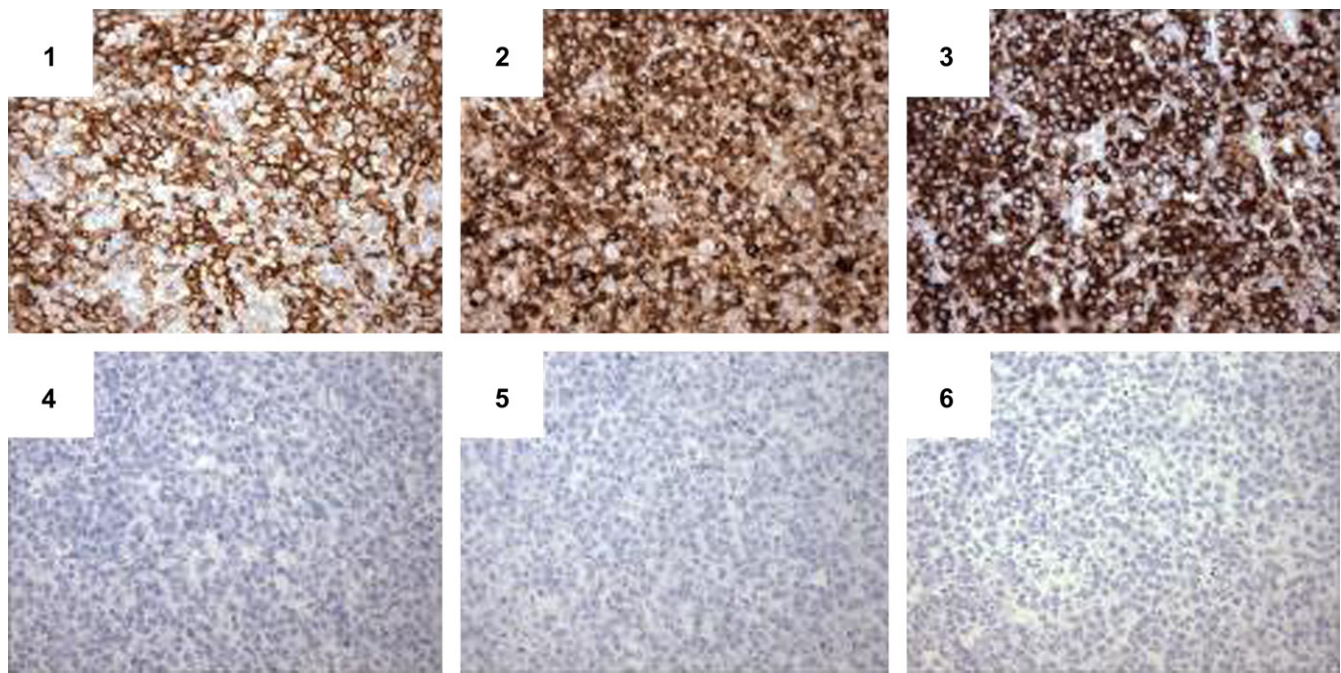


Figure 7. Immunohistochemical analysis for human bone marrow engraftment in severe combined immunodeficient (SCID)-hu mice with BCWM.1 lymphoplasmacytic cells. Immunohistochemical analysis was performed on decalcified fetal bone chips implanted in SCID-hu mice following engraftment with BCWM.1 lymphoplasmacytic cells. Bone chips were retrieved from SCID-hu mice at 12 weeks, following serial detection of rising human paraproteins, and stained with antibodies directed against human CD20 (1), λ light chain (2), IgM (3), κ light chain (4), IgG (5), and IgA (6). Slides viewed at 200 \times magnification.

hybridization studies. However, a vast number of upregulated ($n = 5,409$) and downregulated ($n = 3,155$) genes between BCWM.1 cells and normal donor bone marrow B cells were observed. These differences might reflect epigenetic changes resulting from transforming events, or the differentiation (i.e., lymphoplasmacytic) state of WM cells relative to normal donor BM B cells. Further studies, particularly of genes detected in aberrant B-cell signaling pathways (as described in Table 1) may provide informative clues behind the transforming events in WM.

An important characteristic of BCWM.1 cells is their rapid engraftment in the SCID-hu mice. As with primary WM LPC [26], BCWM.1 cells also required the human BM milieu for their growth and expansion since subcutaneous injection of BCWM.1 cells in SCID mice failed to lead to engraftment. Human serum IgM and λ light chain, as well as soluble CD27, a novel tumor marker for WM [19,20], were readily detectable following engraftment of BCWM.1 cells. The potential use of BCWM.1 engrafted SCID-hu mice as a relevant model for the study of novel WM therapeutics was recently demonstrated by us using the CD70-directed monoclonal antibody SGN-70. BCWM.1 engrafted SCID-hu mice responded to SGN-70 therapy, whereas untreated mice demonstrated continued disease progression [20].

In summary, the BCWM.1 cell line provides a disease appropriate cell system for the study of WM, which in conjunction with the SCID-hu mouse model may be used as

a convenient model for studies focused on both WM pathogenesis and development of targeted therapies for WM.

Acknowledgments

The authors wish to acknowledge and thank John Daley and Susan Lazo at the Dana-Farber Cancer Institute for their help with flow cytometric analysis and cell sorting; Courtney Hyland, Charles Lee and Cynthia Morton from the Cytogenetics Core of Dana-Farber/Harvard Cancer Center; Dr. Maria Ericsson from the Electron Microscopy Core Facility at Harvard Medical School; Drs. Edward Fox, Sigita Jonas Verselis, Changzhong Chen and Maura A. Berkeley from the Microarray Core Facility at the Dana-Farber/Harvard Cancer Center.

Supported by the Bing Fund for Waldenström's macroglobulinemia, a Laurie Strauss Leukemia Foundation Fellowship Award (to D.D.S.), and a National Institutes of Health Career Development Award (K-23CA087977-03) to S.P.T. D.D.S., A.W.H., O.T., X.L., E.H., L.X., J.K., J.L.K., Y.T., B.C. performed cellular and molecular studies. P.T., A.W.H., M.C., and P.N. performed animal studies. A.R.B., Z.R.H., and R.J.M. oversaw specimen collection and clinical data analysis. J.Z. performed bioinformatics analysis. L.M.P., K.C., N.M., S.P.T. designed and oversaw studies.

References

- Owen RG, Treon SP, Al-Katib A, et al. Clinicopathological definition of Waldenström's macroglobulinemia: Consensus Panel Recommendations from the Second International Workshop on Waldenström's macroglobulinemia. *Semin Oncol.* 2003;30:110–115.

2. Harris NL, Jaffe ES, Stein H. A revised European-American classification of lymphoid neoplasms: a proposal from the International Lymphoma Study Group. *Blood*. 1994;84:1361–1392.
3. Harris NL, Jaffe ES, Diebold J, et al. World Health Organization classification of neoplastic diseases of the hematopoietic and lymphoid tissues: report of the Clinical Advisory Committee meeting- Airlie House, Virginia, November 1997. *J Clin Oncol*. 1999;17:3835–3849.
4. Treon SP, Hunter ZR, Aggarwal A, et al. Characterization of familial Waldenstrom's macroglobulinemia. *Ann Oncol*. 2006;17:488–494.
5. Schop RFJ, Kuehl WM, Van Wier SA, et al. Waldenstrom's macroglobulinemia neoplastic cells lack immunoglobulin heavy chain locus translocations but have frequent 6q deletions. *Blood*. 2002;100:2996–3001.
6. Schop RF, Van Wier SA, Xu R, et al. 6q deletion discriminates Waldenstrom macroglobulinemia from IgM monoclonal gammopathy of undetermined significance. *Cancer Genet Cytogenet*. 2006;169:150–153.
7. Xu L, Leleu X, Hunter ZR, et al. Abnormal expression of the plasma cell differentiation factor X-box protein 1 (Xbp-1) in Waldenstrom's macroglobulinemia. *Blood*. 2005;106:1003.
8. Leleu X, Xu L, Ho A, et al. Multiple defects in expression of genes promoting plasmacytic differentiation define Waldenstrom's macroglobulinemia. *Ann Oncol*. 2005;16:v86.
9. Avet-Loiseau H, Garand R, Lode L, Robillard N, Bataille R. 14q32 translocations discriminate IgM multiple myeloma from Waldenstrom's macroglobulinemia. *Semin Oncol*. 2003;30:153–155.
10. Sahota SS, Forconi F, Ottensmeier CH, et al. Typical Waldenström macroglobulinemia is derived from a B-cell arrested after cessation of somatic mutation but prior to isotype switch events. *Blood*. 2002;100:1505–1507.
11. Kriangkum J, Taylor BJ, Treon SP, Mant MJ, Belch AR, Pilarski LM. Clonotypic IgM V/D/J sequence analysis in Waldenstrom macroglobulinemia suggests an unusual B-cell origin and an expansion of polyclonal B cells in peripheral blood. *Blood*. 2004;104:2134–2142.
12. San Miguel JF, Vidrales MB, Ocio E, et al. Immunophenotypic analysis of Waldenstrom's macroglobulinemia. *Semin Oncol*. 2003;30:187–195.
13. Treon SP, Kelliher A, Keele B, et al. Expression of serotherapy target antigens in Waldenström's macroglobulinemia: therapeutic applications and considerations. *Semin Oncol*. 2003;30:243–247.
14. Hunter Z, Branagan AR, Ditzel Santos D, et al. High levels of soluble immunoregulatory receptors in patients with Waldenstrom's macroglobulinemia. *Blood*. 2004;104:303b.
15. Dimopoulos MA, Kyle RA, Anagnostopoulos A, Treon SP. Diagnosis and management of Waldenstrom's macroglobulinemia. *J Clin Oncol*. 2005;23:1564–1577.
16. Hunter ZR, Branagan AR, Manning R, et al. CD5, CD10, CD23 expression in Waldenstrom's macroglobulinemia. *Clin Lymph*. 2005;5:246–249.
17. Ditzel Santos D, Tournilhac O, Xu L, et al. B-Lymphocyte stimulator protein (BLYS) is expressed by bone marrow mast and lymphoplasmacytic cells in Waldenstrom's macroglobulinemia, and provides signaling for growth, survival and IgM secretion. *Blood*. 2004;104:917a.
18. Elsawa SF, Novak AJ, Grote DM, et al. B-lymphocyte stimulator (BLYS) stimulates immunoglobulin production and malignant B-cell growth in Waldenstrom macroglobulinemia. *Blood*. 2006;107:2882–2888.
19. Ho AW, Leleu X, Hatjiharissi E, et al. A novel functional role for soluble CD27 in the pathogenesis of Waldenstrom's macroglobulinemia. *Blood*. 2005;106:4701.
20. Ho AW, Hatjiharissi E, Branagan AR, et al. Therapeutic targeting of CD70 and CD27-CD70 interactions with the monoclonal antibody SGN-70 in Waldenstrom's Macroglobulinemia (WM). *Proc Am Soc Clin Oncol*. 2006;24:102s.
21. Tischendorf W, Hartmann F. Waldenström's macroglobulinemia associated with hyperplasia of the tissue mast cells. *Acta Haematol*. 1950;4:374–383.
22. Wilkins BS, Buchan SL, Webster J, Jones DB. Tryptase-positive mast cells accompany lymphocytic as well as lymphoplasmacytic lymphoma infiltrates in bone marrow trephine biopsies. *Histopathology*. 2001;2:150–155.
23. Santos DD, Chemaly M, Tournilhac O, et al. Bone marrow mast cells are significantly increased in patients with Waldenstrom's macroglobulinemia, and their number following therapeutic intervention is dependent on extent of response. *Blood*. 2005;106:980.
24. Tournilhac O, Santos DD, Xu L, et al. Mast cells in Waldenstrom's macroglobulinemia support lymphoplasmacytic cell growth through CD154/CD40 signaling. *Ann Oncol*. 2006;17:1275–1282.
25. Treon SP, Branagan AR, Hunter Z, et al. IgA and IgG hypogammaglobulinemia persists in most patients with Waldenstrom's macroglobulinemia despite therapeutic responses, including complete remissions. *Blood*. 2004;104:306b.
26. Tassone P, Neri P, Kutok JL, et al. A SCID-hu in vivo model of human Waldenstrom macroglobulinemia. *Blood*. 2005;4:1341–1345.
27. Arens R, Tesselaar K, Baars PA, et al. Constitutive CD27/CD70 interaction induces expansion of effector-type T-cells and results in IFN gamma-mediated B-cell depletion. *Immunity*. 2001;15:801–812.
28. Haiat S, Billard C, Quiney C, Ajchenbaum-Cymbalista F, Kolb JP. Role of BAFF and APRIL in human B-cell chronic lymphocytic leukemia. *Immunology*. 2006;118:281–292.
29. Moreaux J, Legouffe E, Jourdan E, et al. BAFF and APRIL protect myeloma cells from apoptosis induced by interleukin 6 deprivation and dexamethasone. *Blood*. 2004;103:3148–3157.
30. Matsuyama A, Shiraishi T, Trapasso F, et al. Fragile site orthologs FHIT/FRA3B and FHIT/FRA14A2: Evolutionary conserved but highly recombinogenic. *PNAS*. 2003;100:14988–14993.
31. Zhao P, Lam AK, Lu YL, Zhong M, Chen LH, Pu XL. Aberrant FHIT protein expression in classical Hodgkin's lymphoma. *Pathology*. 2006;38:399–402.
32. Kameoka Y, Tagawa H, Tsuzuki S, et al. Contiguous array CHG at 13p14.2 to the FRA3B/FHIT common fragile region as the target gene in diffuse large cell lymphoma. *Oncogene*. 2004;23:9148–9154.